SCIENTIFIC REPORTS

OPEN

SUBJECT AREAS:
BACTERIA
VASCULAR DISEASES

Received
23 April 2013

Accepted
17 March 2014

Published
15 April 2014

Promotion of atherosclerosis by *Helicobacter cinaedi* infection that involves macrophage-driven proinflammatory responses

Shahzada Khan[1]*, H. N. Ashiqur Rahman[2]*, Tatsuya Okamoto[2]*, Tetsuro Matsunaga[3], Yukio Fujiwara[4], Tomohiro Sawa[3], Jun Yoshitake[5], Katsuhiko Ono[6], Khandaker Ahtesham Ahmed[2], Md Mizanur Rahaman[2], Kohta Oyama[2], Motohiro Takeya[4], Tomoaki Ida[3], Yoshiaki Kawamura[7], Shigemoto Fujii[2] & Takaaki Akaike[3]

[1]Gladstone Institutes, University of California, San Francisco, CA 94158, [2]Department of Microbiology, Graduate School of Medical Sciences, Kumamoto University, Kumamoto 860-8556, Japan, [3]Department of Environmental Health Sciences and Molecular Toxicology, Tohoku University Graduate School of Medicine, Sendai 980-8575, Japan, [4]Department of Cell Pathology, Graduate School of Medical Sciences, Kumamoto University, Kumamoto 860-8556, Japan, [5]Center for Development of Advanced Medicine for Dementia, National Center for Geriatrics and Gerontology, Obu 474-8511, Japan, [6]Chemistry Department, Sonoma State University, CA 94928, [7]Department of Microbiology, School of Pharmacy, Aichi Gakuin University, Nagoya 464-8650, Japan.

Correspondence and requests for materials should be addressed to T.A. (takakaik@med.tohoku.ac.jp)

* These authors contributed equally to this work.

Helicobacter cinaedi **is the most common enterohepatic *Helicobacter* species that causes bacteremia in humans, but its pathogenicity is unclear. Here, we investigated the possible association of *H. cinaedi* with atherosclerosis *in vivo* and *in vitro*. We found that *H. cinaedi* infection significantly enhanced atherosclerosis in hyperlipidaemic mice. Aortic root lesions in infected mice showed increased accumulation of neutrophils and F4/80$^+$ foam cells, which was due, at least partly, to bacteria-mediated increased expression of proinflammatory genes. Although infection was asymptomatic, detection of cytolethal distending toxin RNA of *H. cinaedi* indicated aorta infection. *H. cinaedi* infection altered expression of cholesterol receptors and transporters in cultured macrophages and caused foam cell formation. Also, infection induced differentiation of THP-1 monocytes. These data provide the first evidence of a pathogenic role of *H. cinaedi* in atherosclerosis in experimental models, thereby justifying additional investigations of the possible role of enterohepatic *Helicobacter* spp. in atherosclerosis and cardiovascular disease.**

Atherosclerosis is the major cause of many cardiovascular diseases (CVDs)[1]. A widely accepted key player in the initiation and progression of atherosclerosis is the chronic inflammatory response[1,2], but the initiating factor in this chronic inflammation in atherosclerotic tissues is still unclear[3]. The generally accepted paradigm implicates a proinflammatory mechanism involving lipid deposition and chemical modification as the initiator of inflammation in atherosclerotic tissues[1,3,4]. An alternative hypothesis that focuses on microbial factors has emerged during the past decades; it suggests that specific pathogens, such as *Chlamydia pneumoniae*[5], cytomegalovirus[6], herpes simplex virus[7], influenza viruses[8], *Porphyromonas gingivalis*[9], *Aggregatibacter actinomycetemcomitans*[10], *Toxoplasma gondii*[11], and a few other reported pathogens, may be sources of inflammation. However, a number of studies claimed a lack of association of the above-mentioned microbes with the pathogenesis of atherosclerosis[12–15]. Several clinical trials also failed to confirm antibiotic treatment (for *C. pneumoniae* and *Helicobacter pylori*) or prevention through vaccination (for influenza virus) as effective interventions for CVD, which resulted in limited enthusiasm for the belief that microbes are aetiological agents in the pathogenesis of atherosclerosis[3]. Although failure of antibiotic trials suggests that the specific pathogens did not contribute to the disease process, failure may also indicate a lack of antibiotic susceptibility and/or the presence of multiple pathogens in plaque[3,16]. Therefore, the possible role of microbes that are closely related to human habitation, including those yet unidentified in atherosclerosis patients, cannot be ruled out.

Helicobacter cinaedi is the most frequently reported nongastric *Helicobacter* species isolated from both immunocompromised and immunocompetent patients[17,18]. Accumulating evidence suggests that *H. cinaedi* infection may be more common than previously thought because detecting *H. cinaedi* by conventional culture methods is difficult[18–22]. More important, even after successful diagnosis, treatment in many cases seems troublesome because of the growing resistance of *H. cinaedi* to several antibiotics. This resistance often results in failure to eradicate bacteria from infected patients after prolonged therapy[21]. Asymptomatic humans and animals with latent persistent infections have also been reported[23–26]. In fact, a recent study indicated that apparently asymptomatic human carriers may serve as a substantial source of bacterial spread through the faecal-oral route[27].

Many cases of *H. cinaedi* bacteremia were reported in past decades, but clinical manifestations and epidemiology of diseases caused by this bacterium are still unclear[17,18,20]. Evidence suggests that *H. cinaedi* may have particular vascular tropism so that it can cause bacteremia and endovascular infections[28], which are pathological manifestations that do not occur in *H. pylori*-infected patients. In support of such a vascular tropism, Lewis *et al.*[29] reported clinical isolation of *H. cinaedi* from blood of a patient with myopericarditis, and more recently we reported the apparent localization of *H. cinaedi* antigens in human atherosclerotic tissues[25]. Taken together, these clinical observations, if one assumes the possibility of an overlooked laboratory diagnosis, suggest that *H. cinaedi* is a clinically relevant bacterium that may contribute to the development of atherosclerotic CVD. Whether *H. cinaedi* has any pathogenic role in the pathogenesis of atherosclerosis remains unclear, however.

In the present study, we utilized *in vivo* and *in vitro* experimental models to investigate the proatherogenic potential of *H. cinaedi* infection. Pathological and morphometric analyses of aortic tissues showed significantly enhanced development of atherosclerotic lesions in orally infected hyperlipidaemic mice. *H. cinaedi* infection also induced extensive foam cell formation in cultured macrophages and differentiation of THP-1 monocytes into macrophages. These observations warrant additional research to elucidate the aetiological role of *H. cinaedi* and other enterohepatic *Helicobacter* spp. in CVD patients.

Results

Atherosclerosis in the aortic root of *H. cinaedi*-infected B6.Apoe^{shl} mice. B6.Apoe^{shl} mice are spontaneously hyperlipidaemic mice with an apolipoprotein E deficiency and have been utilized to study the development of atherosclerosis[30]. To investigate the involvement of *H. cinaedi* in the pathogenesis of atherosclerosis, we orally infected B6.Apoe^{shl} mice with *H. cinaedi*. All mice were fed a high-cholesterol (1.25%) diet for 8 weeks, and cross-sections of the aortic sinus were stained with Oil Red O for quantification of lesion areas. *H. cinaedi* infection substantially increased the size of atherosclerotic lesions in the aortic sinus compared with that in uninfected control mice (Fig. 1a). To observe and quantify the lipid-rich atherosclerotic plaques in similarly infected mice, aortas from another cohort pair of experimentally infected and control mice were opened longitudinally and stained with Sudan IV, which revealed that *H. cinaedi* infection increased both the number and the size of the atherosclerotic plaques in the aortas, particularly in aortic arch regions (Fig. 1b–g). To evaluate the pathogenic potential of *H. cinaedi* in mouse models that are less susceptible to atherosclerosis development, we similarly infected wild-type (WT) and endothelial nitric oxide synthase deficient (eNOS$^{-/-}$) mice in a separate experiment. However, no atherosclerotic lesions developed in WT and eNOS$^{-/-}$ mice in either infected or control groups during the study period of 8 weeks (Fig. 1c).

Histopathological and immunohistochemical analyses of the aortic sinus. In B6.Apoe^{shl} mice, we found two stages of atherosclerotic lesion development, as determined according to previously reported criteria[9]. The primary stage featured Oil Red O-stained lesions that resembled foam cell lesions. Both infected and control groups had lesions close to the aortic valve attachment site. The infected group had more abundant lesions in the free aortic wall compared with the control group (Fig. 2a). The advanced stage of atherosclerotic lesion development had a mixture of Oil Red O-stained cells, acellular zones, and an inflammatory infiltrate. The infected group had higher number of advanced lesions in both the free aortic walls and the aortic valve attachment region compared with the control group (Fig. 2a). Both infected and control groups demonstrated F4/80 immunostaining of macrophages, but the infected group showed considerably pronounced immunostaining compared with the control group (Fig. 2b). Lesions in infected mice also manifested increased recruitment of neutrophils (Fig. 2c). Enhanced F4/80 immunostaining and neutrophil accumulation in lesions of the infected group indicated enhanced inflammatory changes in the vascular walls of these mice.

Inflammatory gene expression in aortic tissues during *H. cinaedi* infection. To clarify the molecular basis of *H. cinaedi*-induced atherogenic changes in the vascular wall, a separate group of B6.Apoe^{shl} mice was orally infected and their aortic tissues were analysed after 4 weeks of infection. To exclude inflammatory effects of a high-fat diet, these mice were fed a normal chow diet throughout the study period. Gene expression analysis by real-time reverse transcriptase PCR revealed significantly increased expression of inducible NOS (iNOS), interleukin-1β (IL-1β), and Toll-like receptor (TLR) 4 in aortic tissues of infected mice compared with that in control mice ($P < 0.05$) (Fig. 3). C-C motif chemokine 2 (CCL2) and intercellular adhesion molecule-1 (ICAM-1), two prominent mediators responsible for leukocyte adhesion and recruitment in the vascular wall[31,32], were also significantly upregulated in aortas of infected mice ($P < 0.05$) (Fig. 3).

Detection of *H. cinaedi* mRNA and DNA in B6.Apoe^{shl} mice after infection. During the experimental period, no mice had any symptoms of *H. cinaedi* infection such as diarrhea or cellulitis, which are seen in infected patients[17,18,33]. To confirm that *H. cinaedi* infection did indeed occur and to investigate potential sites of bacterial persistence, we attempted to detect *H. cinaedi* mRNA or DNA in various tissues and faecal samples from the same mice that were utilized in the study of inflammatory gene quantification. Blood samples were cultured first in a growth medium to increase the quantity of bacterial DNA for efficient amplification by our recently described nested PCR method[27]. Nested PCR amplified *H. cinaedi* DNA from two (of three) blood culture samples (Fig. 4a). Also, kidney (all three) and faecal (two of three) samples from infected mice contained bacterial DNA (Fig. 4a). No *H. cinaedi* DNA was identified in uninfected control mice (Fig. 4). In addition, immunohistochemical analyses showed the presence of *H. cinaedi* in caecal tissues (see Supplementary Fig. S1 online). This finding indicated successful colonization of the intestinal tract, which may be required for establishment of subsequent persistent infection.

Because bacterial mRNAs are known to have a half-life in seconds to minutes, and therefore detection of bacterial mRNA as well as bacterial DNA has been applied in many studies to identify the live, viable and even metabolically active (i.e., infectious) bacteria in tissue samples[34]. In the present study, analysis of mRNA in aortic tissues by reverse transcription and nested PCR showed amplification of the transcript of the cytolethal distending toxin gene *cdt* of *H. cinaedi* in the infected mice. Because this toxin is known to be a major pathogenic factor of *H. cinaedi*, its mRNA detection strongly indicates the presence of viable and potentially infectious (proliferative) forms of *H. cinaedi* in aortic tissues (Fig. 4b).

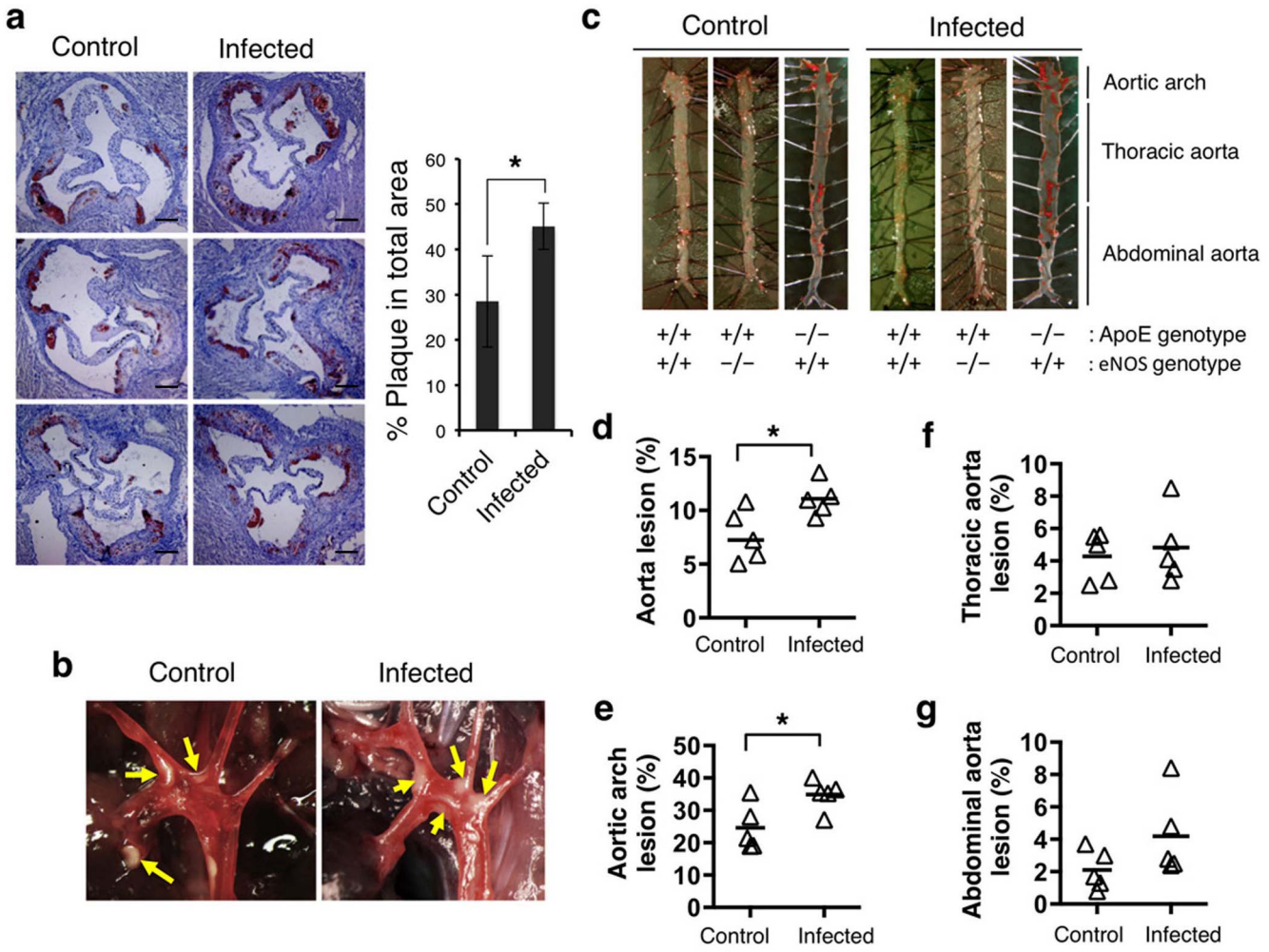

Figure 1 | Oral infection with *H. cinaedi* enhanced atherosclerosis in B6.Apoe^{shl} mice. Mice were killed at 8 weeks after oral infection. (a) Lesions in the aortic sinus stained with Oil Red O (red), and the stained areas were quantified and expressed as % plaque in the total aortic sinus area. Sections were counterstained with haematoxylin. Scale bars, 200 μm. Data are means ± s.d. *$P < 0.05$, n = 5 in each group. (b) Representative photographs of aortic arch regions with white plaques (yellow arrows) in B6.Apoe^{shl} mice. Images are representative of an independent experiment separate from (a) with 5 mice per group. (c) Representative images of Sudan IV-stained (red) aortas from mice with the indicated genotypes. B6.Apoe^{shl} aortas are from mice described in (b). (d–g) Percentages of Sudan IV-stained atherosclerotic plaques in the total aortic areas of B6.Apoe^{shl} mice from (c). *$P < 0.05$.

Although *H. cinaedi* DNA could not be detected in liver and spleen tissues (Fig. 4a), infected mice had a higher ratio of spleen weight to body weight than did control mice (see Supplementary Fig. S2 online). Caecal tissues in infected mice showed mild infiltration of F4/80$^+$ macrophage cells and neutrophils (see Supplementary Fig. S1 online). Shen *et al.* reported similar trend of moderate inflammation responses, e.g., mild typhlocolitis in the cecocolic junction with increased iNOS expression, in B6 and IL-10-defecient mice infected with *H. cinaedi*[35]. The present immunohistochemical analyses also revealed not only strong iNOS expression but also remarkable formation of 8-nitro-cGMP and S-guanylated proteins in caecal tissues in infected mice (cf. Supplementary Fig. S1 online). We identified recently 8-nitro-cGMP as well as protein S-guanylation as prominent biomarkers and mediators for inflammatory responses associate with excessive production of NO (from iNOS in this case) and reactive oxygen species[36–39]. Therefore, though not extensive, appreciable levels of inflammation may occur in caecal tissues, which is considered as a characteristic for *H. cinaedi* infected or the colonized B6 and B6.Apoe^{shl} mice.

Macrophage-derived foam cell formation during *H. cinaedi* infection. We then used a cell culture system to clarify the role of *H. cinaedi* in macrophage-derived foam cell formation (Fig. 5). Peritoneal macrophages from WT mice and human monocyte-derived macrophages (HMDMs) were infected with *H. cinaedi* in the presence or absence of human low-density lipoprotein (LDL). Foam cell formation was assessed by using Oil Red O staining. Only *H. cinaedi*-infected cells accumulated lipid droplets, the hallmark of foam cell formation; uninfected and *H. pylori*-infected cells did not (Fig. 5a). Analysis of cellular lipid contents revealed that *H. cinaedi*-infected macrophages accumulated an increasing number of lipid droplets rich in cholesteryl esters in an infection dose-dependent manner (Fig. 5b and Supplementary Fig. S3a online). Free cholesterol is toxic to cells, which therefore normally convert it to cholesteryl ester for cellular storage in lipid droplets. In fact, as shown in Fig. 5b, the level of free cholesterol did not increase significantly during infection with *H. cinaedi* at an MOI up to 10, whereas the level of cholesteryl ester was elevated even at an infection dose of MOI 1.0. Moreover, lipid droplets found to be accumulated in *H. cinaedi*-infected HMDMs without human LDL added to culture media (Fig. 5c). A similar trend was observed for peritoneal macrophages infected with *H. cinaedi* (data not shown). This result is in clear contrast to the cellular response seen for *C. pneumoniae*-induced foam cells, when infected cells accumulated

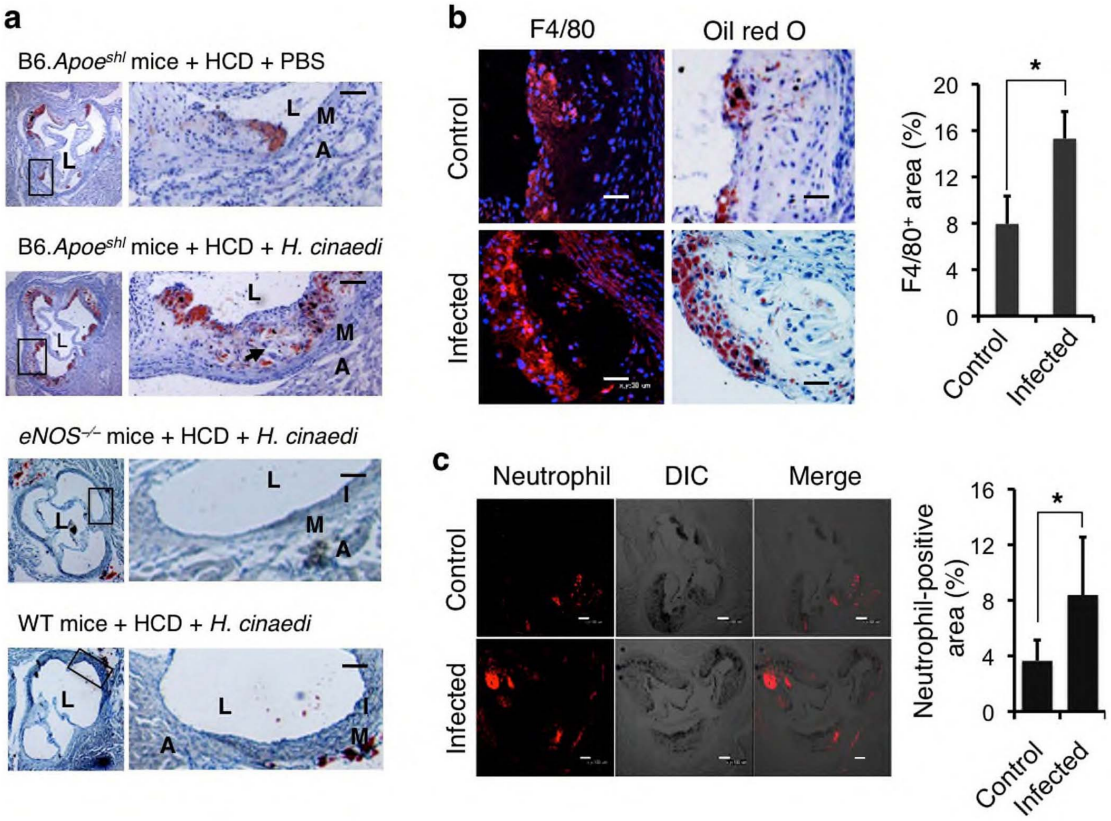

Figure 2 | *H. cinaedi* infection induced advanced atherosclerotic lesion development and enhanced macrophage and neutrophil accumulation in atherosclerotic lesions of B6.Apoe^{shl} mice. Mice were killed at 8 weeks after oral *H. cinaedi* infection. (a) Representative Oil Red O-stained cross-sections of aortic root lesions from *H. cinaedi*-infected mice or PBS-treated mice fed a high-cholesterol diet (HCD) ($n = 5$ in each group). Most lesions in the vehicle-treated mice were adjacent to the valve attachment and were mainly first-stage foam cell lesions. Lesions in *H. cinaedi*-infected mice, however, were more abundant throughout the free aortic wall, had acellular cores (arrow), and represented the advanced stage of atherosclerosis. Proximal aortas of eNOS$^{-/-}$ and WT mice appeared normal after 8 weeks of infection. L, aortic lumen; I, intima; M, media; and A, adventitia. Scale bars in right panels, 20 μm. (b) Serial cross-sections of the aortic sinus of B6.Apoe^{shl} mice showing F4/80 immunostaining and Oil Red O staining of advanced lesions of infected and vehicle-treated control mice ($n = 5$ in each group). Percentages of F4/80-immunostained areas in aortic sinus lesions are also shown. Data are means ice (Scale bars, 30 μm. $^*P < 0.05$. (c) Representative cross-sections of the aortic sinus of B6.Apoe^{shl} mice showing immunostaining of neutrophils ($n = 4$ in each group). The percentage of neutrophil-positive area in the total aortic sinus lesion is shown. Data are means. S. Scale bar, 100 μm. $^*P < 0.05$. DIC, differential interference contrast.

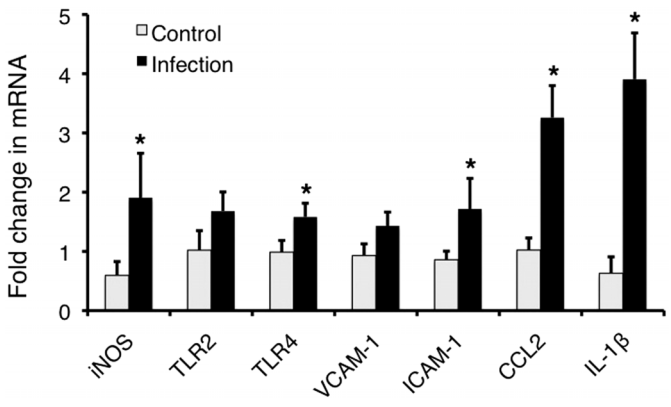

Figure 3 | Relative gene expression levels in aortas of control and infected B6.Apoe^{shl} mice. Mice were orally infected with *H. cinaedi* or sham-treated with PBS (control) and were killed after 4 weeks of feeding a normal chow diet ($n = 3$ in each group). Total RNA from aortic tissues was extracted, and mRNAs were quantified via real-time reverse transcriptase PCR. The relative quantities of experimental mRNA were normalized to the quantity of β-actin mRNA. Data are means ± s.d. $^*P < 0.05$ versus control.

lipid droplets only in the presence of exogenous LDL in culture media; infected cells without exogenous LDL did not transform into foam cells[40].

We further examined the possibility that cholesterol derived by bacteria might have contributed to the foam cell formation in absence of exogenous LDL, utilizing lipoprotein-deficient serum (LPDS) and analyzed foam cell formation by *H. cinaedi*-infected RAW cells. Supplementary Fig. S3b shows that the infected cells did not accumulate lipid droplets when fetal bovine serum (FBS) in the culture media was replaced with LPDS. However, the infected cells started to induce foam cell formation, when LDL was added to the cell culture with LPDS. Standard FBS contains approximately 300 μg/ml cholesterol, consisting partly of LDL cholesterol, according to manufacture's data. Therefore, our observation indicated that *H. cinaedi*-infected macrophages utilized the LDL cholesterol available from the 10% serum in the cell culture media, rather than *H. cinaedi*-derived cholesterol, to accumulate lipid droplets.

Levels of ABCG1 in *H. cinaedi*-infected macrophages. Evidence has suggested critical roles for ATP-binding cassette (ABC) transporters A1 and G1 in macrophage foam cell formation and atherosclerosis development[41,42]. To evaluate the effect of *H. cinaedi* in ABCG1 expression in macrophages/monocytes, therefore, we analysed lysates of infected and uninfected peritoneal macrophages and

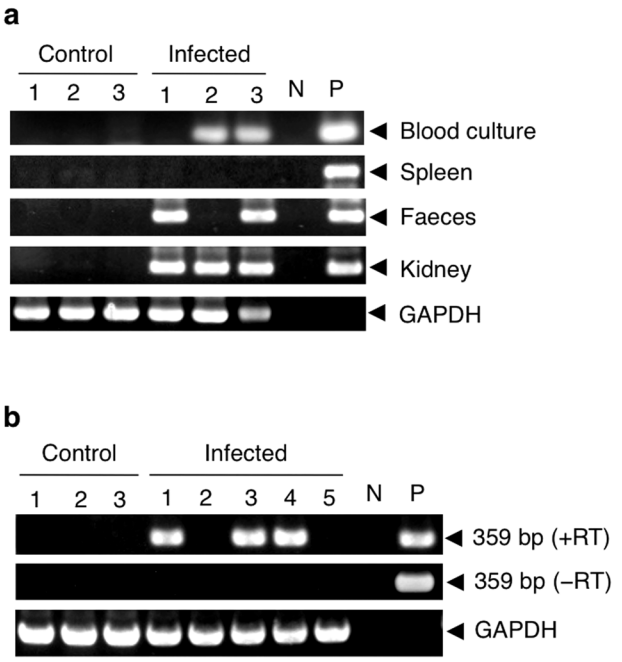

Figure 4 | Nested PCR detection of bacterial DNA and RNA in specimens of *H. cinaedi*-infected and vehicle-treated B6.Apoe^{shl} mice. The nested PCR assay used two pairs of primers that amplify the *cdt* gene of *H. cinaedi* into a 359-bp DNA fragment. Amplification product of mouse glyceraldehyde-3-phosphate dehydrogenase (GAPDH) mRNA was used as a loading control. Each lane indicates an individual mouse. P, PCR-positive control; N, PCR-negative control. (a) The 359-bp region of bacterial *cdt* gene was detected in DNA samples extracted from mouse-specimens at 4 weeks after *H. cinaedi* infection. Vehicle-treated mice had no bacterial *cdt*. All samples had amplifiable host DNA as shown by the representative image for GAPDH PCR. (b) Total RNA from aortic tissue was subjected to reverse transcriptase PCR followed by nested PCR detection of *cdt*. Uncropped gel images are shown in Supplementary Fig. S7.

THP-1 monocyte-derived macrophages by using Western blot analysis. As Figure 6a and b illustrates, *H. cinaedi*-infected mouse peritoneal macrophages and THP-1 monocyte-derived macrophages had significantly reduced levels of ABCG1 ($P < 0.05$). Also, THP-1 monocytes had reduced ABCG1 levels as seen by immunocytochemistry, and the infected cells manifested a morphological change (Fig. 6c). *H. pylori*-infected THP-1 monocyte-derived macrophages, however, had an increase in ABCG1 protein. ABCA1 expression in THP-1 monocyte-derived macrophages was not affected by infection with *H. cinaedi* or *H. pylori* (Fig. 6b). Lipopolysaccharide (LPS) treatment of THP-1 monocyte-derived macrophages produced no apparent change in ABCG1 and ABCA1 expression (Fig. 6b).

Expression of LDL receptor (LDLR) in *H. cinaedi*-infected macrophages. The LDLR on macrophages reportedly played a role in atherosclerotic lesion development in C57BL/6 mice[43]. We found that *H. cinaedi* infection induced significantly increased expression of LDLR protein in HMDMs ($P < 0.05$), with or without the addition of human LDL to the culture medium (Fig. 6d–f). While LDLR expression was likely decreased by exogenous addition of LDL (though not statistically significant), it was significantly attenuated by the treatment with acetylated LDL (AcLDL) in cultured HMDMs. However, *H. cinaedi*-infection obviously upregulated the expression of LDLR (Fig. 6d,e), despite accumulation of cholesteryl ester (Fig. 5b). This finding thus indicates that cholesteryl ester derived from bacteria, if any, did not affect the LDLR expression. On the contrary, infection with a similar dose of *H. pylori* did not increase LDLR expression markedly compared with expression in uninfected control cells (Fig. 6d,e). The class A scavenger receptor SRA1, which binds and takes up AcLDL/oxidized LDL (OxLDL)[44], was downregulated in both *H. cinaedi*- and *H. pylori*-infected HMDMs. The class B scavenger receptor SRB1, which mediates uptake of OxLDL and high-density lipoprotein[45], was unaltered by *H. cinaedi* infection but was markedly upregulated in *H. pylori*-infected cells (Fig. 6d). However, plasma levels of total cholesterol, LDL cholesterol, and triglycerides were unchanged in *H. cinaedi*-infected B6.Apoe^{shl} mice (see Supplementary Fig. S4 online).

All cell cultures were employed at infection doses of *H. cinaedi* below MOI 10, because, at MOI of less than 10, free cholesterol was not increased (Fig. 5b) as well as the cell viability did not decreased, as shown and discussed below. Specifically, the MOI of 0.1 was chosen mostly in the present analyses revealing the notable data shown in Fig. 6. Therefore, we now interpret that the finding of increased expression of LDL receptors coupled with reduced expression of ABCG1 is physiologically relevant. More importantly, the finding presented in Supplementary Fig. S3b, as mentioned above, may strongly support our interpretation that upregulation of LDLR and downregulation of ABCG1 of the culture macrophages induced by *H. cinaedi* infection may be promoting the cellular uptake of LDL cholesterol originated from FBS. In other words, upregulation of LDLR and downregulation of ABCG1 in *H. cinaedi*-infected macrophages indicated that foam cell formation was mediated by altered LDL metabolism (Fig. 6g).

***H. cinaedi* infection-induced differentiation of THP-1 monocytes into macrophages.** As mentioned earlier, the infected mice in this study developed bacteremia (Fig. 4a), which is often seen in *H. cinaedi*-infected patients[18]. During bacteremia, circulating monocytes are exposed to invading bacteria or bacterial components. Available evidence indicates that the circulating monocytes adhere to activated endothelial cells and migrate into sites that are vulnerable to atherosclerotic lesion formation[46]. Therefore, to assess the effect of *H. cinaedi* infection on the differentiation of monocytes, we used THP-1 monocytes and analysed them for macrophage-like morphological changes such as diffused or amoeboid morphology of cells with cytoplasmic vacuoles[47]. Figure 7a shows representative Giemsa-stained and differential interference contrast (DIC) microscopic images of THP-1 cells at 5 days after infection with *H. cinaedi*. PBS-treated control cells maintained a round shape and apparently had a high nucleus-to-cytoplasm ratio. In contrast, cells infected with viable *H. cinaedi* as well as positive control cells stimulated with phorbol myristate acetate (PMA) showed an obvious change to diffused and enlarged morphology with cytoplasmic vacuoles. Cells treated with heat-killed *H. cinaedi* had only a minimal morphological change, as did cells treated with LPS (Fig. 7b). However, treatment with heat-killed *H. cinaedi* bacteria increased the attachment phenomenon of THP-1 cells compared with that in vehicle-treated cells (see Supplementary Fig. S5a online). Infection with live *H. cinaedi* led to reduction in total number of THP-1 cells (cf. Supplementary Fig. S5b online), which may support our findings related to infection-induced morphological differentiation. Regarding the potentially toxic effect of free cholesterol, the cells were likely suffered from its cytotoxicity only at MOI of 50, where their viability was attenuated (Supplemental Fig. S5c) and the free cholesterol level was elevated (Fig. 5b). However, decrease in cell number at MOI 10 in Supplemental Fig. S5b probably was not due to cytotoxicity of free cholesterol, but rather because of growth inhibition associated with advanced differentiation of THP-1 cells to foam cells. In fact, at MOI of less that 10, free cholesterol was not increased (Fig. 5b) as well as the cell viability did not decreased (Supplemental Fig. S5c). Treatment of cells with Pam3CSK4, a TLR2 ligand[48], resulted in an attachment phenomenon and macrophage-like morphology close to

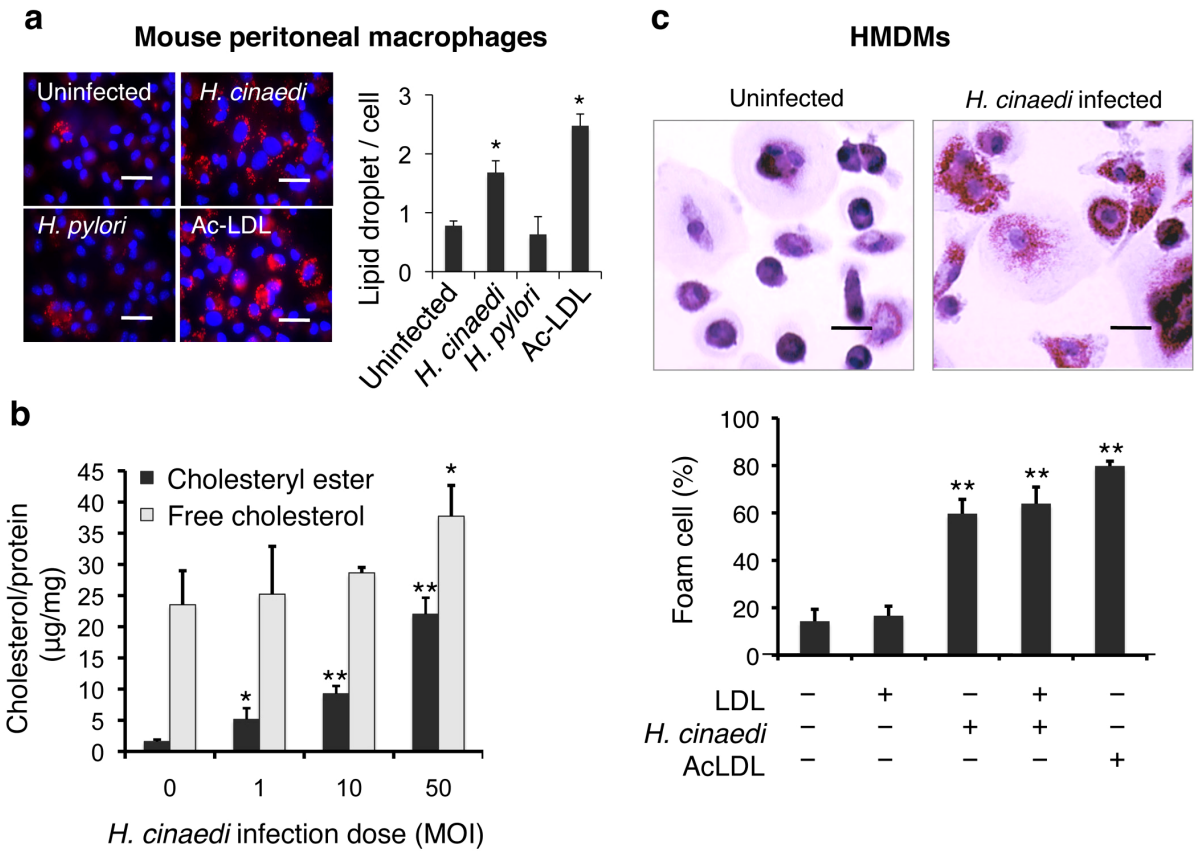

Figure 5 | *H. cinaedi* induced macrophage foam cell formation *in vitro*. (a) Oil Red O staining of peritoneal macrophages from WT mice infected with *H. cinaedi* or *H. pylori* at an MOI of 0.1 for 24 h, and the number of Oil Red O-positive lipid droplets per cell. Macrophages treated with acetylated LDL (AcLDL) (50 μg ml^{-1}) were used as a positive control for foam cell formation. Nuclei were stained with DAPI. Scale bars, 20 μm. (b) Cholesterol content of peritoneal macrophages infected with different doses of *H. cinaedi*. (c) Oil Red O staining of HMDMs infected for 24 h with *H. cinaedi* (0.1 MOI) in the presence or absence of human LDL, and the percentage of foam cells. Cells were counterstained with haematoxylin. Scale bars, 10 μm. In all experiments cells were cultured in the medium containing 10% fetal bovine serum. Data are means ± s.d. from a representative experiment ($n = 3$). *$P < 0.05$, **$P < 0.01$ versus uninfected cells.

those of the heat-killed *H. cinaedi*-treated cells (Fig. 7a,b). Pretreatment of THP-1 cells with TLR2 or TLR4 neutralizing antibodies significantly inhibited *H. cinaedi*-induced morphological differentiation ($P < 0.05$) (Fig. 7c), which indicated the involvement of these two TLRs. Finally, assessment of macrophage marker expression by Western blot analysis and immunocytochemistry revealed that *H. cinaedi*-infected THP-1 cells had an increased CD14 level compared with that in uninfected cells (see Supplementary Fig. S6 online). Expression of ICAM-1 also increased in THP-1 cells in an *H. cinaedi* infection dose-dependent manner (see Supplementary Fig. S6 online).

Discussion

Our current study reports that *H. cinaedi*, a difficult-to-detect and emerging enterohepatic pathogen, enhanced the development of atherosclerosis in hyperlipidaemic mice. This increased atherosclerosis in *H. cinaedi*-infected mice was associated with activation of proatherogenic pathways, as evidenced by increased accumulation of macrophage foam cells and neutrophils in atherosclerotic lesions. Successful identification of *H. cinaedi* mRNA in aortic tissues of infected mice indicated the presence of bacteria, although infection was apparently asymptomatic. Our cell culture studies with peritoneal macrophages, THP-1 cells, and HMDMs indicated that *H. cinaedi* infection altered the expression of cholesterol receptors or transporters and caused foam cell formation, which is a hallmark of atherosclerosis progression. These observations, combined with our previous report on immunohistochemical detection of *H. cinaedi* in human atherosclerotic tissues[25], suggested a close association of *H. cinaedi* with atherosclerosis in infected individuals. Further investigations will be required to determine whether *H. cinaedi* plays a causative role in development of atherosclerosis in infected patients.

H. cinaedi has been primarily isolated from immunocompromised patients with various clinical manifestations, such as meningitis, bacteremia, cellulitis, enteritis, and was less commonly isolated from patients with no recognized defect in host defense[17,18,20]. Our recent study[27] however, revealed that *H. cinaedi* is likely colonized in the intestinal tract among healthy individuals, who may be then affected asymptomatically with its persistent infection. Therefore, we sought to clarify any pathological and clinical consequences of a possible persistent infection of *H. cinaedi* focusing on its potential to develop atherosclerosis.

For the present study, we administered *H. cinaedi* orally, as a natural route of infection, because our recent research identified the DNA of *H. cinaedi* in faeces from healthy volunteers and *H. cinaedi*-infected patients, which suggested a faecal-oral route of transmission[27]. For *H. cinaedi* identification in infected mice, we detected mRNA and DNA derived from *cdt* gene of *H. cinaedi* by using nested PCR assay we recently established[27] (Fig. 4), because *H. cinaedi* is difficult to be isolated effectively via conventional bacterial culture especially with small amounts of tissue specimens (e.g., mouse aorta) due to the fastidious and slowly growing nature of this microaerobic bacteria as we reported earlier[18,19,27]. Although the present mouse model of *H. cinaedi* infection was apparently asymptomatic in view of severe clinical manifestations due to typical enteritis

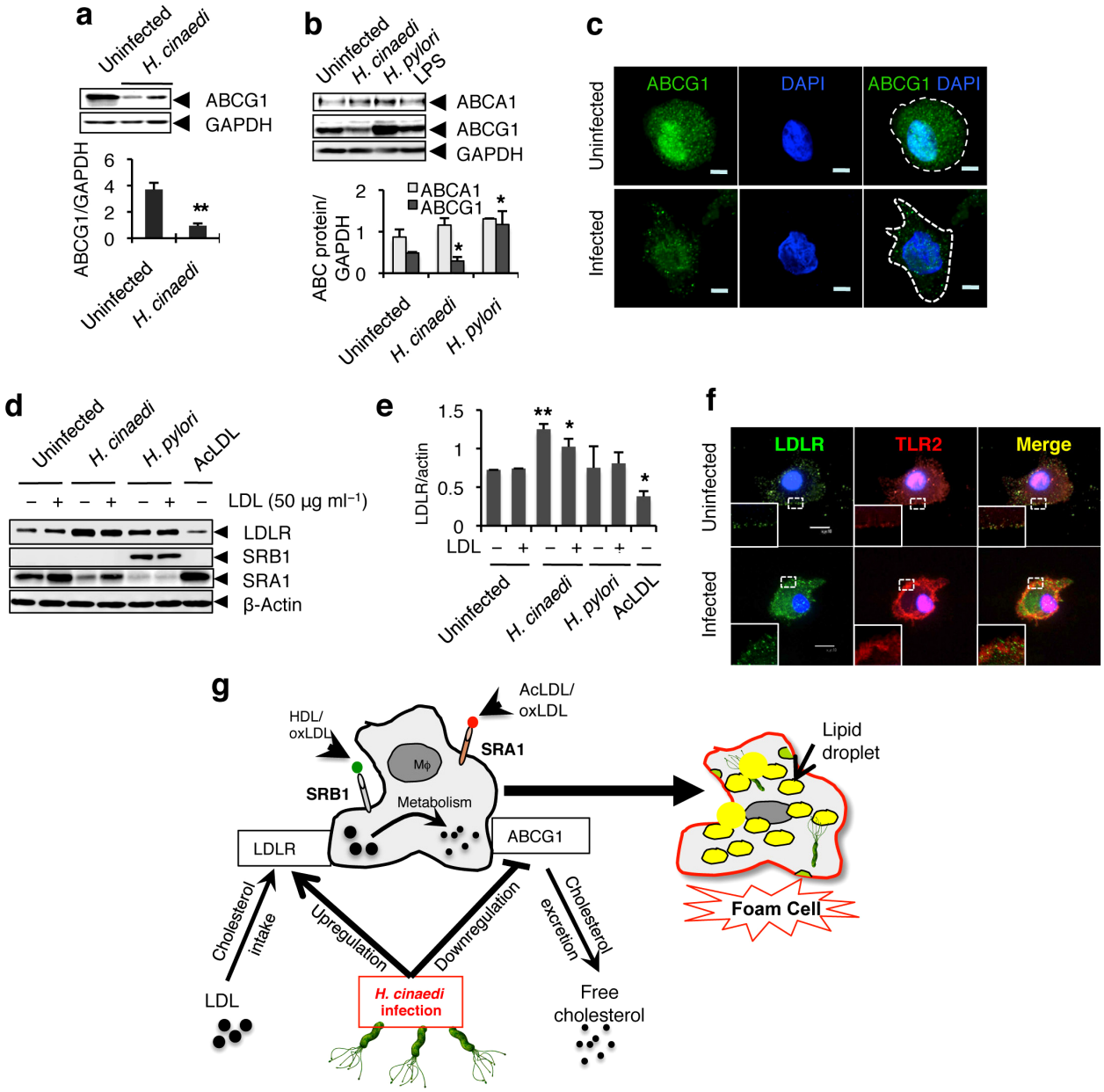

Figure 6 | ABCG1 was downregulated and LDLR was upregulated in *H. cinaedi*-infected macrophages. Western blot analysis of whole-cell lysates of (a) WT peritoneal macrophages and (b) THP-1 monocyte-derived macrophages infected with the indicated bacteria at an MOI of 0.1 or treated with *Escherichia coli* LPS (100 ng ml^{-1}) for 24 h. Data are means ± s.d. from a representative experiment ($n = 3$). *$P < 0.05$, **$P < 0.01$ versus the PBS-treated control. (c) THP-1 monocytes were infected with *H. cinaedi* at an MOI of 0.1 for 5 days or were uninfected, and ABCG1 was detected by immunohistochemistry. Scale bar, 5 μm. (d) Western blot analysis of whole-cell lysate protein from HMDMs infected with the indicated bacteria (0.1 MOI) or treated as indicated for 24 h. (e) Quantification of the densitometric measurement of relative band intensity of mature LDLR from the Western blot. (f) Representative fluorescent confocal images showing expression of LDLR and TLR2 in HMDMs infected with *H. cinaedi* (0.1 MOI) or treated with vehicle for 24 h. Scale bars, 10 μm. In all experiments (a to f) cells were cultured in the medium containing 10% fetal bovine serum. (g) Schematic representation of *H. cinaedi*-induced foam cell formation mechanism. Uncropped blots (a, b, and d) are shown in Supplementary Fig. S8.

(e.g., diarrhea) and septicemia, the finding of *H. cinaedi* mRNA as well as its DNA identified unequivocally in either aortic or other tissues of infected mice is considered to be indicative of bacterial live cell activities indeed present *in vivo* in mice infected with *H. cinaedi* (Fig. 4). This interpretation was further supported by clear evidence of inflammatory responses in systemic as well as vascular lesions (Figs. 3 and S1). In fact, detection of *H. cinaedi* mRNA and DNA in aorta and blood culture samples of infected mice in this study (Fig. 4), together with an earlier report of recurrent bacteremia in patients[18], may reflect the vascular tropism of *H. cinaedi* and its ability to cause systemic infection. The presence of bacterial mRNA and DNA in samples collected at 4 weeks after infection also indicated that *H. cinaedi* caused a chronic infection in these experimental mice. Therefore, chronic systemic dissemination of bacteria or bacterial components and active infection of aortic tissues may have directly caused proinflammatory gene expression in vascular walls (Fig. 3) and promoted the progression of atherosclerosis (Figs. 1 and 2).

The results of this study do not necessarily prove direct causality, however, because the B6.Apoe^{shl} mice that we used have a preexisting genetic risk factor for atherosclerosis. Also, our current finding of no atherosclerotic lesions in WT and eNOS$^{-/-}$ mice fed

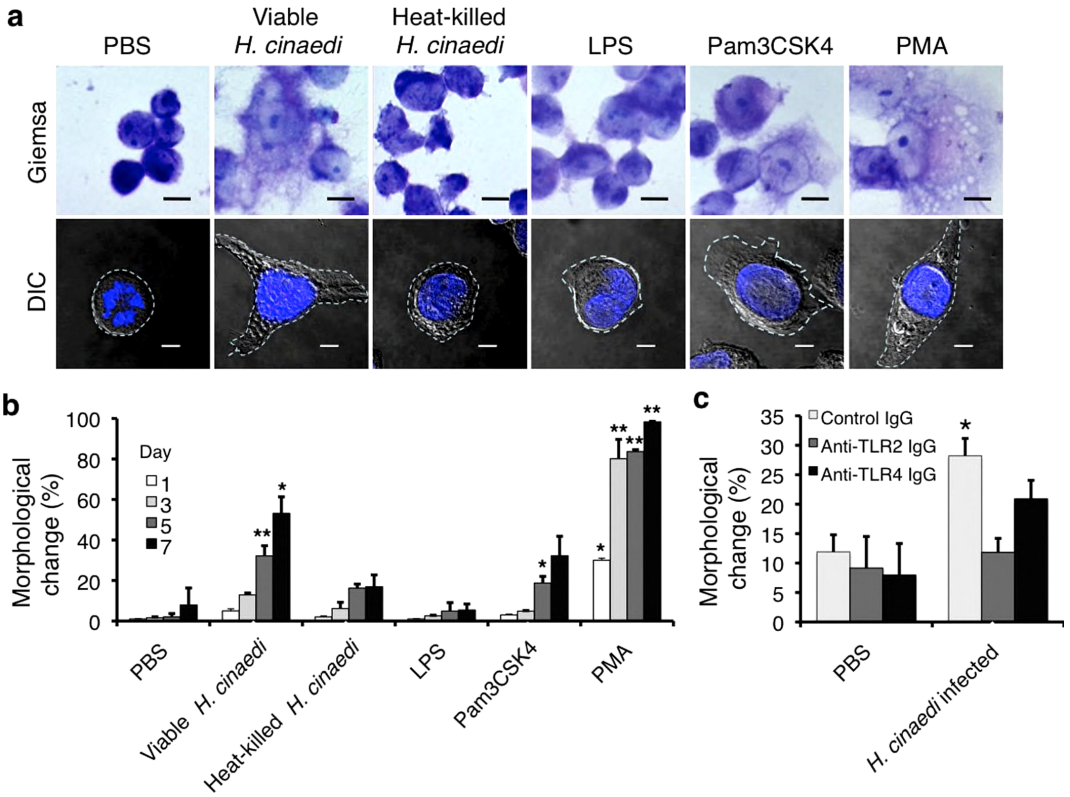

Figure 7 | *H. cinaedi* induced morphological differentiation of THP-1 monocytes. Suspended THP-1 cells were seeded in eight-well glass chamber slides and were infected with viable or heat-killed *H. cinaedi* at an MOI of 0.1 or were treated with *E. coli* LPS (100 ng ml^{-1}), Pam3CSK4 (100 ng ml^{-1}), or PMA (100 nM) for up to 7 days. (a) Representative bright-field images of Giemsa-stained cells and DIC images are shown at day 5 after infection or treatment. Scale bars in the Giemsa panel, 20 μm; scale bars in the DIC panel, 5 μm. (b) Percentages of cells with macrophage-like morphology, i.e., diffused or amoeboid shapes and cytoplasmic vacuoles, as shown by Giemsa staining, at the indicated time points. (c) Cells were treated with control isotype IgG or anti-TLR2 or anti-TLR4 IgG antibodies for 3 h and were then infected with live *H. cinaedi* (0.1 MOI) for 3 days. Percentages of morphologically changed cells were determined after Giemsa staining. For (b) and (c), at least 100 Giemsa-stained cells were counted manually at each time point for each treatment. In all experiments (a to c) cells were cultured in the medium containing 10% fetal bovine serum. Experiments were performed in triplicate. Data are means ± s.d. from a representative experiment ($n = 3$). *$P < 0.05$, **$P < 0.01$ versus PBS-treated cells.

a high-cholesterol diet at 8 weeks after *H. cinaedi* infection (Fig. 1c) emphasizes the importance of genetic susceptibility. Earlier studies reported that WT and eNOS$^{-/-}$ mice rarely developed atherosclerotic lesions during the short period of study[49,50]. In addition to genetic factors, another risk factor that was recently described is phosphatidylcholine metabolites that are generated by the metabolic activity of gut flora[51]. To maintain the natural intestinal habitat, we did not eliminate (e.g., with antibiotic treatment) the existing normal gut flora of animals in this study. Determination of changes in intestinal flora, if any, that occur because of *H. cinaedi* infection is an important subject that warrants future investigations. Regarding the association of bacterial infection with atherosclerosis, Koren *et al.* performed some molecular epidemiological analysis with microbiota of oral cavity, gut, and atherosclerotic plaques from patients with atherosclerosis by using the pyrosequencing of the bacterial 16S rRNA gene[52]. In their study, any particular 16S rRNA gene-associated PCR amplicon was not listed for *Helicobacter* species. However, earlier reports suggest that comparison of the near-complete 16S rRNA gene sequences may have also led to incorrect identification of *H. cinaedi*, until a full genome sequencing that we and others completed recently[27,53]. Therefore, it may be possible that the *H. cinaedi* gene might have been overlooked and remains mostly uncertain. In any events, a notable atherosclerosis promoting potential of *H. cinaedi* is clarified herein, which further support the atherosclerosis pathogenesis involving polymicrobial mechanism to cause chronic inflammatory response in human vasculatures. In fact, additional epidemiological studies of atherosclerosis patients are needed to determine the cause-and-effect relationship in humans. Nonetheless, the results of this study demonstrate a potential of *H. cinaedi* for enhancement of atherosclerosis and provide mechanistic insights into *H. cinaedi*-related atherosclerosis (Fig. 8).

Given the well-known functions of macrophage foam cells in the initiation and progression of atherosclerosis[2], the enhanced foam cell accumulation found here (Fig. 2b) can be considered a key event in the enhancement of atherosclerotic plaque development in infected B6.Apoe^{shl} mice (Fig. 1). Our current cell culture studies also confirmed a direct role of *H. cinaedi* in macrophage foam cell formation (Fig. 5 and Supplementary Fig. S3 online). In our earlier study[25], we clearly demonstrated the presence of *H. cinaedi* antigens in CD68^{+} foam cells in human atherosclerotic tissues. These observations together suggest a causative role of *H. cinaedi* in macrophage foam cell formation during development of atherosclerosis in humans. However, additional studies are required to prove this hypothesis.

In our study here, *H. cinaedi*-infection markedly reduced the level of the cholesterol efflux-related protein ABCG1 in mouse peritoneal macrophages and THP-1 monocyte-derived macrophages (Fig. 6a–c). ABCG1 serves a critical function in the homeostasis of cholesterol metabolism, with an ultimate impact on monocyte-endothelial cell interaction[54], plasma high-density lipoprotein level[55], macrophage apoptosis[56], and atherosclerosis development[57]. Therefore, the ability of *H. cinaedi* to downregulate ABCG1 in macrophages may be a pathophysiologically relevant mechanism for *H. cinaedi*-induced foam cell formation.

H. cinaedi infection substantially upregulated the expression of LDLR protein in HMDMs (Fig. 6d–f), although plasma levels of total cholesterol, LDL cholesterol and triglycerides were unchanged in *H. cinaedi*-infected B6.Apoe^{shl} mice (see Supplementary Fig. S4 online). *H. cinaedi* infection had no significant effect on the expression of SRA1 and SRB1 (Fig. 6d), two scavenger receptors for modified LDL[4]. These results suggested that *H. cinaedi*-induced foam cell formation involves modulation of unmodified LDL metabolism. Li *et al.* reported a similar finding of increased macrophage LDLR expression in response to acute inflammation[58]. Infection of HMDMs with *H. pylori*, however, did not significantly alter the expression of LDLR along with SRA1, whereas it caused significantly increased expression of SRB1 in our study ($P < 0.05$) (Fig. 6d). Expression of ABCG1 and ABCA1 also markedly increased in *H. pylori*-infected THP-1 monocyte-derived macrophages (Fig. 6b). These contrasting effects of *H. pylori* and *H. cinaedi* on cholesterol receptors and transporters explain in part why macrophages infected with *H. pylori* did not transform into foam cells (Fig. 5a). Despite the same genus of these two bacterial species, their effects on cellular lipid metabolism appear to be distinct because of pathogenic characteristics that are yet to be elucidated.

H. cinaedi infection also led to differentiation of THP-1 monocytes, which depended mainly on TLR2/TLR4 signalling (Fig. 7c). TLR signalling reportedly played important roles in both murine and human atherosclerosis[48,59]. In our study, *H. cinaedi*-infected mice showed increased mRNA expression of both TLR2 and TLR4 in aortic tissues (Fig. 3), which suggests the involvement of these two pattern recognition receptors in *H. cinaedi*-related atherosclerosis. However, detailed investigations, perhaps utilizing gene knockout macrophages and mouse models, are required to confirm the role of individual TLRs in *H. cinaedi*-induced monocyte differentiation, macrophage foam cell formation, and atherosclerosis enhancement in mice.

H. cinaedi possesses several virulence factors that may contribute to its pathogenic role in atherosclerosis. According to our recent report[53], the complete genome sequence of *H. cinaedi* indicates the presence of several virulence factors such as cytolethal distending toxin (CDT), alkyl hydroperoxide reductase, neutrophil activation protein, invasion antigen B, a potential type VI secretion system (T6SS), clustered regularly interspaced short palindromic repeats (CRISPR), and CRISPR-associated (Cas) systems. Shen *et al.* showed that CDT was an important factor for *H. cinaedi*-induced typhlocolitis in interleukin-10-deficient mice[35]. This toxin from other bacteria such as *Campylobacter jejuni* and *Helicobacter hepaticus* was also suggested to operate in immune modulation and persistent bacterial colonization in mice[60,61]. Therefore, CDT of *H. cinaedi* may contribute to bacterial persistence in hosts, which is often found in *H. cinaedi*-infected patients[21,22]. However, further investigations are necessary to explore the exact pathogenic role of virulence factors of *H. cinaedi* in the context of atherosclerosis.

In summary, *H. cinaedi* infection significantly enhanced the development of atherosclerosis in spontaneously hyperlipidaemic mice. Increased expression of proinflammatory genes, increased accumulation of neutrophils, and induction of macrophage-derived foam cell formation underlie the pathogenic mechanism of enhanced atherosclerosis, which may be mediated directly by *H. cinaedi* bacteria invading the vasculature. Even though our study does not present evidence of direct causal effects, our findings provide the first data demonstrating the association of *H. cinaedi* with the enhancement of atherosclerosis. Additional investigations to determine the aetiological/contributing role of *H. cinaedi* and other enterohepatic *Helicobacter* spp. in atherosclerotic CVD development are thus warranted.

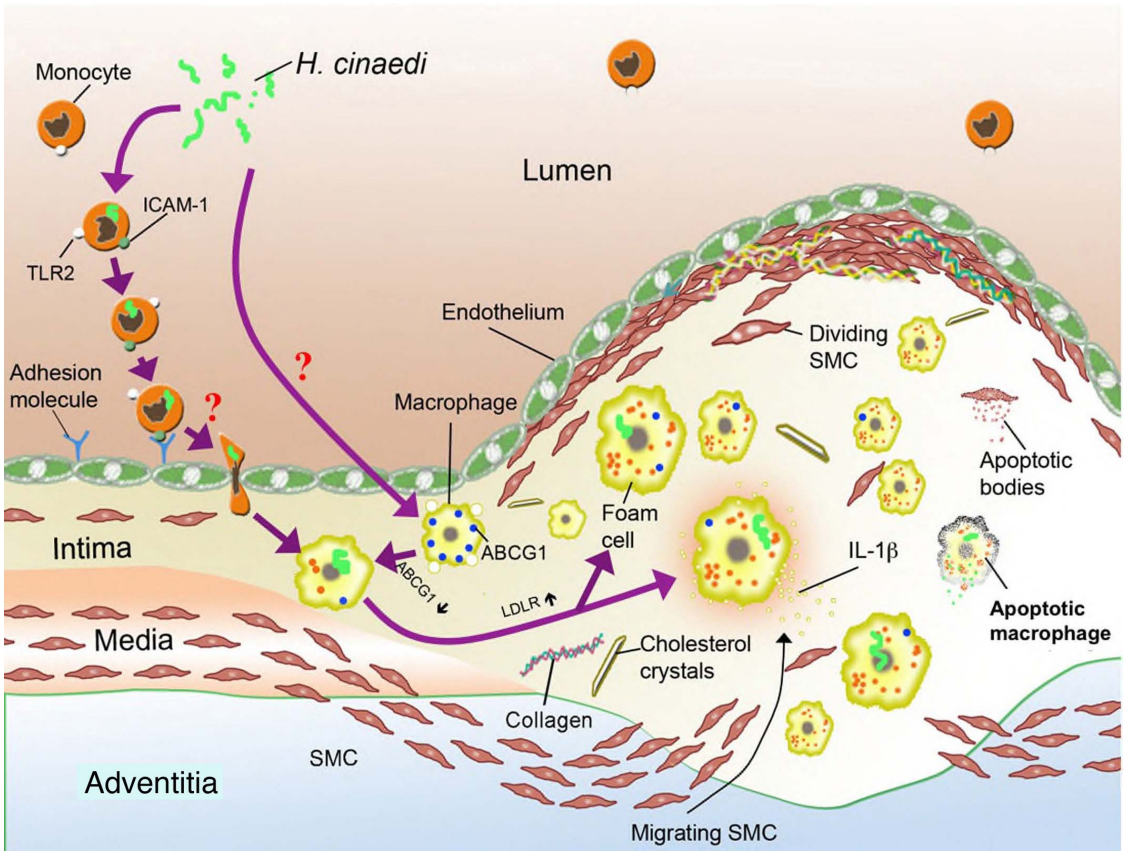

Figure 8 | Schematic representation of the proposed mechanism of *H. cinaedi*-related atherosclerosis. SMC, smooth muscle cell.

Methods

Bacterial culture. A clinical isolate of *H. cinaedi* (strain PAGU 0616)[18,19] was used throughout these studies. *H. cinaedi* and *H. pylori* were grown as described in Supplementary Information online. Heat-killed *H. cinaedi* bacteria were prepared by incubating a bacterial suspension in PBS at 70°C for 30 min. For infection studies, late log-phase bacterial inoculum doses were adjusted by measuring the optical density of the bacterial suspension at 620 nm.

Animals and oral challenge with *H. cinaedi*. All protocols for animal experiments using mice were approved by the Animal Care and Use Committee, Kumamoto University. *H. cinaedi* infection was produced in mice in compliance with the institutional guidelines and regulations, with an effort to minimize the number of animals used and their suffering. WT C57BL/6 mice were purchased from CLEA Japan, Inc. (Tokyo, Japan). eNOS$^{-/-}$ (C57BL/6-Nos3^{tm1unc}) mice were purchased from Jackson Laboratories (West Grove, PA, USA). Spontaneous hyperlipidaemic mice, C57BL/6.KOR-*Apoe*^{shl} (B6.Apoe^{shl}) mice[30], were purchased from Japan SLC (Shizuoka, Japan). All mice were maintained on a standard chow diet and were housed in the Center for Animal Resources and Development, Kumamoto University. Mice of each genotype were divided into two groups: infection and control, with each group comprising five 6- to 8-week-old male mice. Animals were infected with *H. cinaedi* according to the method by Shen Z. *et al*[35] with a slight modification. They established this protocol for infection of B6 and IL10$^{-/-}$ mice with *H. cinaedi* and followed up the infected mice until 12 and 36 weeks postinfection, respectively, and showed via PCR method that colonization peaks at 12 weeks postinfection in B6 mice[35]. In our experiment, briefly, each mouse in the infection groups received 10^9 CFU of live *H. cinaedi* in 200 µl of PBS at pH 7.4 in each oral dose. The infection groups received three doses of *H. cinaedi* in the first week, and a fourth dose in the fourth week of the study period. Mice in control groups were mock-treated with PBS. Throughout the study period, mice were fed a high-fat diet with a high cholesterol level (1.25%). All mice were killed 8 weeks after the initial oral challenge. Before their death, mice were fasted for 16 h. Blood and tissue samples were collected for analysis. The *in vivo* experiments for *H. cinaedi* infection were repeated at least five times with different cohort designs containing more than fifty B6.Apoe^{shl} mice (with or without a high-cholesterol diet) subjected to the various pathological analyses at each time point after infection. This repetitional experimental design was employed to ensure precision and reproducibility of our current *in vivo* study, as described in detail in Supplementary Materials and Methods.

Pathological assessment of atherosclerotic lesions. The heart and proximal section of the aorta were removed from the mice and cleaned of fat and adventitial tissue. The top halves of the hearts were fixed in 4% paraformaldehyde at 4°C and were embedded in Tissue-Tek optimal cutting temperature (OCT) compound (Miles, Elkhart, IN, USA). Atherosclerotic plaque formation was analysed according to the method previously described[62–65] with modifications. Briefly, the aortic root area was identified by the proximal presence of aortic valve leaflets. For preparing the cryosections of aortic sinus, an experienced pathologist (Y.F., coauthor of this paper) blinded to the identity of samples decided the start and end points of aortic sinus based on the morphology of sections under a light microscope. Consecutive sections (7 µm thick) in an entire aortic root area were obtained and mounted serially on ten different slides each numbered from 1 to 10. By the end of sampling/mounting, each slide had ten sections each separated by 70 µm tissue distance. The same numbered slide from each mouse was used for Oil red O staining. To evaluate the lesions, eight sections — four at the end of the aortic sinus and four at the junction between the aortic sinus and the ascending aorta, and each section mounted on the same slide was separated by 70 µm (7 µm/section × 10 slides) in the original tissue — were used for the analysis according to the protocol published by Yagyu *et al*[62]. The sections were stained with Oil Red O and counterstained with haematoxylin. Whole aortas were collected and stained with Sudan IV. ImageJ software (NIH) was used to measure total lumen area including the intimal layer of the aortic sinus, toal area of whole aorta and the areas of atherosclerotic plaques. The plaque area was then divided with the area of aortic lumen or the whole aorta, and the resultant value was expressed as percentage of atherosclerotic plaque area. GraphPad Prism 6.0 (GraphPad Software Inc, San Diego, CA) was used to generate the graphs showing atherosclerotic lesion percentages between control and infection groups of mice.

Nested PCR for detection of *H. cinaedi* DNA from faecal, tissue, and blood specimens. To detect bacterial DNA via a nested PCR assay and to investigate the gene expression profile in aortic tissues, we performed a separate experiment with three control and five infected B6.Apoe^{shl} mice that were fed a normal chow diet for 4 weeks. Mice were infected with *H. cinaedi* as described above, except they did not receive the fourth dose at week 4. All mice were fasted overnight and then were killed after faecal samples were collected. At the time of their death, blood samples were collected aseptically by means of orbital lobe puncture, and the remaining blood was washed away by injecting 10 ml of PBS into the left ventricle to flush out the systemic circulation. Specimens of liver, kidney, spleen, aorta, and caecal tissues were sequentially collected while maintaining the strictest possible aseptic conditions to avoid DNA contamination among specimens.

DNA from these specimens was extracted by using commercially available kits (Qiagen, Valencia, CA, USA). The extracted DNA was then used for a nested PCR assay, as previously described[27], to detect the *cdt* gene of *H. cinaedi*. Because the sensitivity of detection by nested PCR was at least 10^2 CFU ml^{-1} of biological sample[27], we initially cultured freshly collected blood for 3 days in BHI media according to the protocol for bacterial culture as described above. We then centrifuged the cultured blood specimens at 5,000 × *g* for 5 min, and the resultant pellets were subjected to DNA extraction and nested PCR.

RNA isolation from aortas and amplification by real-time reverse transcriptase PCR. Total RNA from aortic tissues was extracted with TRIzol reagent (Invitrogen, Carlsbad, CA, USA) followed by DNase I treatment. The extracted RNA was then reverse-transcribed into cDNA by using random primers (Takara Bio, Otsu, Japan) and was subjected to PCR amplification. Levels of the following inflammatory markers were analysed by using PCR: iNOS, TLR2, TLR4, VCAM-1, ICAM-1, CCL2, and IL-1β. All primers were designed via Primer3plus[66]. Primer sequences (see Supplementary Table S1 online) and other details of the real-time PCR method are described in the Supplementary Information online.

Cell treatments and *H. cinaedi* infection. HMDMs, peritoneal macrophages, and THP-1 monocyte-derived macrophages were cultured in RPMI 1640 with 10% fetal bovine serum all through the experiments. For foam cell-related studies, *H. cinaedi* or *H. pylori* bacteria suspended in PBS were added to these cells at the desired MOI. Cells were then incubated for 24 h with or without human LDL (50 µg ml^{-1}) (Intracel, Frederick, MD, USA). After 24 h of infection or treatments, cells were washed twice with PBS and used for analysis. Preparation of macrophages and other details of cell treatments appear in the Supplementary Information online.

Monocyte differentiation studies. THP-1 cells (1×10^5 cells per well) were seeded in eight-well glass chamber slides and incubated overnight before being used in experiments. *H. cinaedi* bacteria suspended in PBS were added at the desired MOI, or the cells were treated with TLR ligands as described above followed by incubation at 37°C with 5% CO_2 for 1, 3, 5, and 7 days. To observe the attachment phenomenon, suspended and attached cells were collected separately, followed by counting with an automated cell counter (Invitrogen). For morphological analysis, cells were fixed with paraformaldehyde, gently washed twice with PBS, stained with 2% Giemsa (Merck, Darmstadt, Germany), and viewed under a microscope at × 400 magnification. At least 100 cells were counted in five separate fields to determine the percentage of morphologically changed cells. Morphological alterations included a change in cell shape from round to amoeboid, an apparent change in the nucleus-to-cytoplasm ratio, and the presence of cytoplasmic vacuoles. In some experiments, cells were treated for 3 h with neutralizing antibodies against TLR2 and TLR4 (BioLegend, San Diego, CA) at a concentration of 10 mg ml^{-1} and were then infected or treated as described.

Lipid body staining and foam cell analysis. Cells were fixed in 4% buffered formalin for 10 min, washed in distilled water, rinsed in 60% isopropanol, and stained with 0.2% Oil Red O for 15 min. Stained cells were then cleaned in 60% isopropanol and were counterstained with haematoxylin. The aqueous mounting agent Aquatex (Merck, Summit, NJ, USA) was used to mount cells for light microscopic observations. For fluorescence analysis, cells were mounted in 10% glycerol in 20 mM Tris-HCl (pH 7.4) with 4′,6-diamidino-2-phenylindole (DAPI). Foam cells were observed via light or fluorescence microscopy (excitation wavelength 510–560; emission wavelength 575–590) at × 400 magnification with a Nikon Eclipse E1000 microscope (Nikon, Tokyo, Japan). Cells with more than 10 lipid droplets were defined as foam cells and the percentage of foam cells formed in each condition was determined according to a previously described method[67]. The lipid content of macrophages was also determined by means of a colorimetric method. Details of the procedure can be found in the Supplementary Information online.

Confocal microscopy. For all microscopic studies, cells were grown in glass chamber slides and were stimulated or infected as described. Caecal and aortic sinus tissues from the mice were fixed and embedded in OCT according to the procedure described earlier in the section on pathological assessment of atherosclerotic lesions. For determining infiltration of inflammatory cells, sections were stained with either rat anti-mouse anti-neutrophil antibody, clone 7/4, (ABD Serotec, Oxford, UK), or with rat anti-mouse F4/80 antibody (ABD Serotec, Oxford, UK) for macrophage staining. For confirming colonization of *H. cinaedi* in the intestinal tract, cecal tissues from infected and uninfected mice were similarly fixed and stained with a rabbit polyclonal antibody raised against a 30 kDa major antigenic protein of *H. cinaedi*[19,25]. Additional details of the immunostaining procedure are given in the Supplementary Information online. Stained cells and tissues were then examined with a Nikon Eclipse TE2000-E (and Nikon EZ-C1 software) laser scanning confocal microscope (Nikon) with a × 100 oil-immersion objective. Images were edited via ImageJ software and Adobe Photoshop CS4 version 11 (Adobe Systems, Waltham, MA, USA).

Western blot analysis. Cells were lysed in an ice-cold lysis buffer containing 20 mM Tris-HCl (pH 8.0), 140 mM NaCl, 10% glycerol, 1% NP-40, 100 mM NaF, 1 mM Na_3OV_4, and protease inhibitor cocktail (cOmplete ULTRA Tablets, Mini, Roche, Manheim, Germany). Cell lysates (10 µg) were subjected to immunoblot analysis as described in the Supplementary Information online.

Statistical analysis. Statistical significance was defined as $P < 0.05$ in a two-tailed Student's *t*-test. Analyses were performed by means of PASW Statistics, Version 18 (SPSS, Chicago, IL, USA).

1. Libby, P., Ridker, P. M. & Hansson, G. K. Inflammation in atherosclerosis: from pathophysiology to practice. *J. Am. Coll. Cardiol.* **54**, 2129–2138 (2009).
2. Tabas, I. Macrophage death and defective inflammation resolution in atherosclerosis. *Nat. Rev. Immunol.* **10**, 36–46 (2010).
3. Rosenfeld, M. E. & Campbell, L. A. Pathogens and atherosclerosis: update on the potential contribution of multiple infectious organisms to the pathogenesis of atherosclerosis. *Thromb. Haemost.* **106**, 858–867 (2011).
4. Hansson, G. K. & Hermansson, A. The immune system in atherosclerosis. *Nat. Immunol.* **12**, 204–212 (2011).
5. Moazed, T. C., Kuo, C., Grayston, J. T. & Campbell, L. A. Murine models of *Chlamydia pneumoniae* infection and atherosclerosis. *J. Infect. Dis.* **175**, 883–890 (1997).
6. Hsich, E. *et al.* Cytomegalovirus infection increases development of atherosclerosis in apolipoprotein-E knockout mice. *Atherosclerosis* **156**, 23–28 (2001).
7. Alber, D. G., Powell, K. L., Vallance, P., Goodwin, D. A. & Grahame-Clarke, C. Herpesvirus infection accelerates atherosclerosis in the apolipoprotein E-deficient mouse. *Circulation* **102**, 779–785 (2000).
8. Naghavi, M. *et al.* Influenza infection exerts prominent inflammatory and thrombotic effects on the atherosclerotic plaques of apolipoprotein E-deficient mice. *Circulation* **107**, 762–768 (2003).
9. Li, L., Messas, E., Batista, E. L., Jr., Levine, R. A. & Amar, S. *Porphyromonas gingivalis* infection accelerates the progression of atherosclerosis in a heterozygous apolipoprotein E-deficient murine model. *Circulation* **105**, 861–867 (2002).
10. Zhang, T. *et al.* *Aggregatibacter actinomycetemcomitans* accelerates atherosclerosis with an increase in atherogenic factors in spontaneously hyperlipidemic mice. *FEMS Immunol. Med. Microbiol.* **59**, 143–151 (2010).
11. Portugal, L. R. *et al.* Infection with *Toxoplasma gondii* increases atherosclerotic lesion in ApoE-deficient mice. *Infect. Immun.* **72**, 3571–3576 (2004).
12. Daus, H. *et al.* Lack of evidence for a pathogenic role of *Chlamydia pneumoniae* and cytomegalovirus infection in coronary atheroma formation. *Cardiology* **90**, 83–88 (1998).
13. Ayada, K. *et al.* Chronic infections and atherosclerosis. *Ann. N. Y. Acad. Sci.* **1108**, 594–602 (2007).
14. Brenner, H., Berg, G., Frohlich, M., Boeing, H. & Koenig, W. Chronic infection with *Helicobacter pylori* does not provoke major systemic inflammation in healthy adults: results from a large population-based study. *Atherosclerosis* **147**, 399–403 (1999).
15. Morre, S. A., Stooker, W., Lagrand, W. K., van den Brule, A. J. & Niessen, H. W. Microorganisms in the aetiology of atherosclerosis. *J. Clin. Pathol.* **53**, 647–654 (2000).
16. Epstein, S. E., Zhu, J., Najafi, A. H. & Burnett, M. S. Insights into the role of infection in atherogenesis and in plaque rupture. *Circulation* **119**, 3133–3141 (2009).
17. Fox, J. G. The non-*H pylori* helicobacters: their expanding role in gastrointestinal and systemic diseases. *Gut* **50**, 273–283 (2002).
18. Kitamura, T. *et al.* *Helicobacter cinaedi* cellulitis and bacteremia in immunocompetent hosts after orthopedic surgery. *J. Clin. Microbiol.* **45**, 31–38 (2007).
19. Iwashita, H. *et al.* Identification of the major antigenic protein of *Helicobacter cinaedi* and its immunogenicity in humans with *H. cinaedi* infections. *Clin. Vaccine Immunol.* **15**, 513–521 (2008).
20. Solnick, J. V. Clinical significance of *Helicobacter* species other than *Helicobacter pylori*. *Clin. Infect. Dis.* **36**, 349–354 (2003).
21. Uckay, I. *et al.* Recurrent bacteremia with *Helicobacter cinaedi*: case report and review of the literature. *BMC Infect. Dis.* **6**, 86 (2006).
22. Vandamme, P., Harrington, C. S., Jalava, K. & On, S. L. Misidentifying helicobacters: the *Helicobacter cinaedi* example. *J. Clin. Microbiol.* **38**, 2261–2266 (2000).
23. Fernandez, K. R., Hansen, L. M., Vandamme, P., Beaman, B. L. & Solnick, J. V. Captive rhesus monkeys (*Macaca mulatta*) are commonly infected with *Helicobacter cinaedi*. *J. Clin. Microbiol.* **40**, 1908–1912 (2002).
24. Fennell, C. L. *et al.* Characterization of *Campylobacter*-like organisms isolated from homosexual men. *J. Infect. Dis.* **149**, 58–66 (1984).
25. Khan, S. *et al.* Potential association of *Helicobacter cinaedi* with atrial arrhythmias and atherosclerosis. *Microbiol. Immunol.* **56**, 145–154 (2012).
26. Totten, P. A. *et al.* *Campylobacter cinaedi* (sp. nov.) and *Campylobacter fennelliae* (sp. nov.): two new *Campylobacter* species associated with enteric disease in homosexual men. *J. Infect. Dis.* **151**, 131–139 (1985).
27. Oyama, K. *et al.* Identification of and screening for human *Helicobacter cinaedi* infections and carriers via nested PCR. *J. Clin. Microbiol.* **50**, 3893–3900 (2012).
28. van der Ven, A. J., Kullberg, B. J., Vandamme, P. & Meis, J. F. *Helicobacter cinaedi* bacteremia associated with localized pain but not with cellulitis. *Clin. Infect. Dis.* **22**, 710–711 (1996).
29. Lewis, G. D., Holmes, C. B., Holmvang, G. & Butterton, J. R. Case records of the Massachusetts General Hospital. Case 8-2007. A 48-year-old man with chest pain followed by cardiac arrest. *N. Engl. J. Med.* **356**, 1153–1162 (2007).
30. Matsushima, Y., Hayashi, S. & Tachibana, M. Spontaneously hyperlipidemic (SHL) mice: Japanese wild mice with apolipoprotein E deficiency. *Mamm. Genome* **10**, 352–357 (1999).
31. Linton, M. F. & Fazio, S. Macrophages, inflammation, and atherosclerosis. *Int. J. Obes. Relat. Metab. Disord.* **27 Suppl 3**, S35–40 (2003).
32. Nakashima, Y., Raines, E. W., Plump, A. S., Breslow, J. L. & Ross, R. Upregulation of VCAM-1 and ICAM-1 at atherosclerosis-prone sites on the endothelium in the ApoE-deficient mouse. *Arterioscler. Thromb. Vasc. Biol.* **18**, 842–851 (1998).
33. Cuccherini, B. *et al.* Bacteremia and skin/bone infections in two patients with X-linked agammaglobulinemia caused by an unusual organism related to *Flexispira*/*Helicobacter* species. *Clin. Immunol.* **97**, 121–129 (2000).
34. Rayner, M. G. *et al.* Evidence of bacterial metabolic activity in culture-negative otitis media with effusion. *JAMA* **279**, 296–299 (1998).
35. Shen, Z. *et al.* Cytolethal distending toxin promotes *Helicobacter cinaedi*-associated typhlocolitis in interleukin-10-deficient mice. *Infect. Immun.* **77**, 2508–2516 (2009).
36. Sawa, T. *et al.* Protein *S*-guanylation by the biological signal 8-nitroguanosine 3′,5′-cyclic monophosphate. *Nat. Chem. Biol.* **3**, 727–735 (2007).
37. Zaki, M. H. *et al.* Cytoprotective function of heme oxygenase 1 induced by a nitrated cyclic nucleotide formed during murine salmonellosis. *J. Immunol.* **182**, 3746–3756 (2009).
38. Nishida, M. *et al.* Hydrogen sulfide anion regulates redox signaling via electrophile sulfhydration. *Nat. Chem. Biol.* **8**, 714–724 (2012).
39. Ito, C. *et al.* Endogenous nitrated nucleotide is a key mediator of autophagy and innate defense against bacteria. *Mol. Cell* **52**, 794–804 (2013).
40. Cao, F., Castrillo, A., Tontonoz, P., Re, F. & Byrne, G. I. *Chlamydia pneumoniae*-induced macrophage foam cell formation is mediated by Toll-like receptor 2. *Infect. Immun.* **75**, 753–759 (2007).
41. Aiello, R. J. *et al.* Increased atherosclerosis in hyperlipidemic mice with inactivation of ABCA1 in macrophages. *Arterioscler. Thromb. Vasc. Biol.* **22**, 630–637 (2002).
42. Meurs, I. *et al.* The effect of ABCG1 deficiency on atherosclerotic lesion development in LDL receptor knockout mice depends on the stage of atherogenesis. *Atherosclerosis* **221**, 41–47 (2012).
43. Herijgers, N., Van Eck, M., Groot, P. H., Hoogerbrugge, P. M. & Van Berkel, T. J. Low density lipoprotein receptor of macrophages facilitates atherosclerotic lesion formation in C57Bl/6 mice. *Arterioscler. Thromb. Vasc. Biol.* **20**, 1961–1967 (2000).
44. Fong, L. G. & Le, D. The processing of ligands by the class A scavenger receptor is dependent on signal information located in the cytoplasmic domain. *J. Biol. Chem.* **274**, 36808–36816 (1999).
45. Valacchi, G., Sticozzi, C., Lim, Y. & Pecorelli, A. Scavenger receptor class B type I: a multifunctional receptor. *Ann. N. Y. Acad. Sci.* **1229**, E1–7 (2011).
46. Tacke, F. & Randolph, G. J. Migratory fate and differentiation of blood monocyte subsets. *Immunobiology* **211**, 609–618 (2006).
47. Yamaguchi, H., Haranaga, S., Widen, R., Friedman, H. & Yamamoto, Y. *Chlamydia pneumoniae* infection induces differentiation of monocytes into macrophages. *Infect. Immun.* **70**, 2392–2398 (2002).
48. Mullick, A. E., Tobias, P. S. & Curtiss, L. K. Modulation of atherosclerosis in mice by Toll-like receptor 2. *J. Clin. Invest.* **115**, 3149–3156 (2005).
49. Campbell, L. A., Blessing, E., Rosenfeld, M., Lin, T. & Kuo, C. Mouse models of *C. pneumoniae* infection and atherosclerosis. *J. Infect. Dis.* **181 Suppl 3**, S508–513 (2000).
50. Shesely, E. G. *et al.* Elevated blood pressures in mice lacking endothelial nitric oxide synthase. *Proc. Natl. Acad. Sci. USA* **93**, 13176–13181 (1996).
51. Wang, Z. *et al.* Gut flora metabolism of phosphatidylcholine promotes cardiovascular disease. *Nature* **472**, 57–63 (2011).
52. Koren, O. *et al.* Human oral, gut, and plaque microbiota in patients with atherosclerosis. *Proc. Natl. Acad. Sci. USA* **108**, 4592–4598 (2011).
53. Goto, T. *et al.* Complete genome sequence of *Helicobacter cinaedi* strain PAGU611, isolated in a case of human bacteremia. *J. Bacteriol.* **194**, 3744–3745 (2012).
54. Whetzel, A. M. *et al.* ABCG1 deficiency in mice promotes endothelial activation and monocyte-endothelial interactions. *Arterioscler. Thromb. Vasc. Biol.* **30**, 809–817 (2010).
55. Wiersma, H. *et al.* Lack of Abcg1 results in decreased plasma HDL cholesterol levels and increased biliary cholesterol secretion in mice fed a high cholesterol diet. *Atherosclerosis* **206**, 141–147 (2009).
56. Baldan, A. *et al.* Impaired development of atherosclerosis in hyperlipidemic Ldlr$^{-/-}$ and ApoE$^{-/-}$ mice transplanted with Abcg1$^{-/-}$ bone marrow. *Arterioscler. Thromb. Vasc. Biol.* **26**, 2301–2307 (2006).
57. Out, R. *et al.* Macrophage ABCG1 deletion disrupts lipid homeostasis in alveolar macrophages and moderately influences atherosclerotic lesion development in LDL receptor-deficient mice. *Arterioscler. Thromb. Vasc. Biol.* **26**, 2295–2300 (2006).
58. Li, L., Thompson, P. A. & Kitchens, R. L. Infection induces a positive acute phase apolipoprotein E response from a negative acute phase gene: role of hepatic LDL receptors. *J. Lipid Res.* **49**, 1782–1793 (2008).
59. Monaco, C. *et al.* Toll-like receptor-2 mediates inflammation and matrix degradation in human atherosclerosis. *Circulation* **120**, 2462–2469 (2009).
60. Fox, J. G. *et al.* Gastroenteritis in NF-kB-deficient mice is produced with wild-type *Camplyobacter jejuni* but not with *C. jejuni* lacking cytolethal distending toxin despite persistent colonization with both strains. *Infect. Immun.* **72**, 1116–1125 (2004).

61. Pratt, J. S., Sachen, K. L., Wood, H. D., Eaton, K. A. & Young, V. B. Modulation of host immune responses by the cytolethal distending toxin of *Helicobacter hepaticus*. *Infect. Immun.* **74**, 4496–4504 (2006).
62. Yagyu, H. *et al.* Overexpressed lipoprotein lipase protects against atherosclerosis in apolipoprotein E knockout mice. *J. Lipid Res.* **40**, 1677–1685 (1999).
63. Allen, J. M., Thompson, G. R., Myant, N. B., Steiner, R. & Oakley, C. M. Cardiovascular complications of homozygous familial hypercholesterolaemia. *Br. Heart J.* **44**, 361–368 (1980).
64. Nakashima, Y., Plump, A. S., Raines, E. W., Breslow, J. L. & Ross, R. ApoE-deficient mice develop lesions of all phases of atherosclerosis throughout the arterial tree. *Arterioscler. Thromb.* **14**, 133–140 (1994).
65. Tangirala, R. K., Rubin, E. M. & Palinski, W. Quantitation of atherosclerosis in murine models: correlation between lesions in the aortic origin and in the entire aorta, and differences in the extent of lesions between sexes in LDL receptor-deficient and apolipoprotein E-deficient mice. *J. Lipid Res.* **36**, 2320–2328 (1995).
66. Untergasser, A. *et al.* Primer3Plus, an enhanced web interface to Primer3. *Nucleic Acids Res.* **35**, W71–74 (2007).
67. Schaffner, T. *et al.* Arterial foam cells with distinctive immunomorphologic and histochemical features of macrophages. *Am. J. Pathol.* **100**, 57–80 (1980).

Acknowledgments

We thank Judith B. Gandy for her excellent editing of the manuscript. This work was supported in part by a Grant-in-Aid for Challenging Exploratory Research (grant number 21659109) from the Ministry of Education, Culture, Sports, Science and Technology (MEXT), Japan. S.K. was supported by the Japanese Government Scholarship (Monbukagakusho, MEXT) for doctoral studies.

Author contributions

S.K., H.N.A.R., T.O. and T.A. designed the experiments, performed the analyses, and wrote the paper. Y.F. and M.T. helped with cell biology, gene expression analyses, and mouse studies. T.M., K.Ono and K.Oyama performed nested PCR analyses. J.Y., K.A.A., M.M.R. and H.N.A.R. provided technical help with immunochemical and immunoblot analyses. T.S., T.I., S.F. and Y.K. performed data analyses and edited the paper. T.A. supervised the study.

Additional information

Supplementary information accompanies this paper at http://www.nature.com/scientificreports

Competing financial interests: The authors declare no competing financial interests.

How to cite this article: Khan, S. *et al.* Promotion of atherosclerosis by *Helicobacter cinaedi* infection that involves macrophage-driven proinflammatory responses. *Sci. Rep.* **4**, 4680; DOI:10.1038/srep04680 (2014).